# A universal method for camera calibration in UITS scenes

**Zhaoxue Chen (陈兆学) and Pengfei Shi (施鹏飞)**

*Institute of Image Processing and Pattern Recognition, Shanghai Jiaotong University, Shanghai 200030*

Received June 23, 2004

A universal approach to camera calibration based on features of some representative lines on traffic ground is presented. It uses only a set of three parallel edges with known intervals and one of their intersected lines with known slope to gain the focal length and orientation parameters of a camera. A set of equations that computes related camera parameters has been derived from geometric properties of the calibration pattern. With accurate analytical implementation, precision of the approach is only decided by accuracy of the calibration target selecting. Final experimental results have showed its validity by a snapshot from real automatic visual traffic surveillance (AVTS) scenes.

*OCIS codes:* 100.6890, 100.0100, 100.2000.

Automatic visual traffic surveillance (AVTS) plays an important role in urban intelligent transportation systems (UITSs), which can contribute to rich traffic information in intuition during the course of traffic scene analysis such as traffic light status, tracks or speed of different vehicles, license plate or vehicle dimension information and occurrence of traffic accidents, etc.. For most applications in an effective AVTS, camera calibration is a crucial and fundamental step, which determines the mapping relationship between the two-dimensional (2D) camera image coordinates and the 3D world coordinates[1,2].

There are many different approaches existed for camera calibration. A typical one is to use the sets of corresponding points in the world coordinates and in the image coordinates to derive the camera parameters[3]. It is very inconvenient to measure a large amount of data with respect to the world frame by this approach. Therefore another kind of approach is widely adopted by utilizing some special calibration targets or special image features to replace the measurement of corresponding points. For such methods, convenient feature extraction or selection of an efficient calibration object is an essential step. In Ref. [4], Bas and Crisman proposed an easy to install camera calibration for traffic monitoring. In their method, neither measuring corresponding points nor special calibration targets were required. By selecting the road edges in an image, the vanishing point of the road edge was used to compute the focal length and pan angle of the camera. However, they assumed the height and the tilt angle of the camera beforehand. Obviously, using predefined parameters of the camera is not practical in some applications and unmatched with an excellent camera calibration method. Wang *et al.*[5] employed a hexagon with 3 pairs of parallel edges as the calibration target to generate a vanishing line of the ground plane from its image. Their idea is proved to be an efficient way for camera calibration. However, when it comes to traffic scenes, it is nearly impossible to find a regular hexagon, which is a great limit. In Ref. [2], Yung *et al.* introduced a novel calibration method for traffic video surveillance system based on the geometric properties of four corners of a rectangle determined by the road lane on the road surface. By their approach the orientation, position, and focal length of the camera could be simply resolved in linear time. It is no doubt that their method is efficient and superior to traffic camera calibration, however, different from what they said, the calibration rectangle is still not so easy to be found in some occasions such as the traffic surveillance scenes of urban intersections, which is a fly in the ointment. After investigating some easy-to-got characteristics of urban traffic scenes, we introduce a new universal method for camera calibration based on arrangement information of some special lines on the traffic ground plane. Instead of a regular rectangle, this method needs only a set of three parallel edges with known intervals and a line with known slope both in the world and their corresponding projection in the image to gain the focal length and the orientation parameters of the camera. The distance between two adjacent parallel lines is measured beforehand and the intersected line with known slope is selected from the scene ahead of time. In real occasions, such features as zebra lines or lanes include two roadside edges may be good choices for the required parallel lines set, which are representative in traffic scenes and the line with known slope is also not very difficult to be chosen or set, which assures the universality of the method in UITS scenes.

The calibration target in this paper is a set of three parallel edges with known intervals and a intersecting line of them with known slope, as shown in Figs. 1(a) and (b), which is represented by $a$, $b$, $c$, $d$ in the world and $a'$, $b'$, $c'$, $d'$ on the image, respectively. Here the slope of line $d$ is measured as $m$ beforehand and the distance between two adjacent lines of lines $a$, $b$, $c$ is supposed to be known as $d_1$, $d_2$ in sequence. Line $\overline{V_D V_0}$ in Fig. 1(a) denotes the vanishing line of the ground plane and point $V_D$, $V_0$ represents the vanishing point of lines $a$, $b$, $c$ and line $d$ respectively.

To calibrate the camera orientation and the focal length parameters, two right-handed coordinate systems need to be defined, i.e., the world coordinate system and the camera centered one. Suppose the origin of the world coordinate system is located at the intersection point $O$ of lines $b$ and $d$ with the positive $Y$ axis pointing forward along $b$, the positive $Z$ axis being vertical to the ground pointing upward and positive $X$ axis pointing rightward.

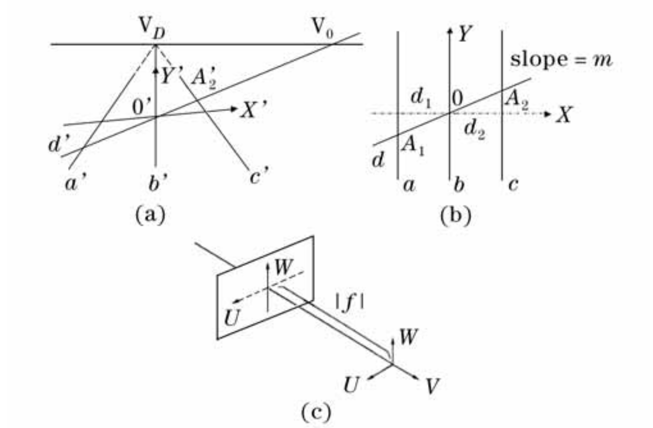


Fig. 1. The calibration target (a) and the world system (b), and the camera coordinate system (c).

The camera coordinate system with the lens center as the origin is shown in Fig. 1(c). The $V$ axis is the optical axis of the camera and the $U-W$ plane is parallel to the image plane located at $V=f$ with $f$ being the negation of the camera focal length. The image coordinates of any point in the image plane are specified as $(u,w)$ with respect to the camera coordinate system[5].

Suppose the camera lens center is located at ($x_c$, $y_c$, $z_c$), and pan, tilt, and swing angles of the camera are $\theta$, $\varphi$, $\psi$, respectively, then the coordinate transformation between the two coordinate systems defined above can be written as

$$(u,v,w,1)=(x,y,z,1)\cdot T^{-1}\cdot M, \tag{1}$$

where $T=\begin{bmatrix}1&0&0&0\\0&1&0&0\\0&0&1&0\\x_c&y_c&z_c&1\end{bmatrix}$, $M=\begin{bmatrix}A&D&G&0\\B&E&H&0\\C&F&I&0\\0&0&0&1\end{bmatrix}$, $A=\cos\theta\cos\psi+\sin\theta\sin\phi\sin\psi$, $B=\sin\theta\cos\psi-\cos\theta\sin\phi\sin\psi$, $C=\cos\phi\sin\psi$, $D=-\sin\theta\cos\phi$, $E=\cos\theta\cos\phi$, $F=\sin\phi$, $G=\sin\theta\sin\phi\cos\psi-\cos\theta\sin\psi$, $H=-\cos\theta\sin\phi\cos\psi-\sin\theta\sin\psi$, and $I=\cos\phi\cos\psi$.

Considering a ground point $(x,y,0)$ in the world coordinate system, its projected point in the image is $(u,w)$, and the equation can be derived as[5]

$$x_c=x+h(uA+fD+wG)/(uC+fF+wI), \tag{2}$$

where $h$ is mounting height of the camera.

Then, from Eq. (2), the projection line of a ground line parallel to the $Y$ axis in the world coordinate system can be represented in the image as

$$\left(A-\frac{x_c-d}{h}C\right)u+\left(G-\frac{x_c-d}{h}I\right)w$$
$$+\left(D-\frac{x_c-d}{h}F\right)f=0, \tag{3}$$

where $d$ is a constant and represents the corresponding intercept of the line on $x$ axis.

According to perspective geometry, the parallel lines in 3D can be thought to meet at infinity. The projection of this point onto the image plane is called "vanishing point"[4]. Therefore, as shown in Fig. 1(a), lines $a'$, $b'$, $c'$ must be converging at a vanishing point $V_D$ with public coordinates[5]

$$(u_D,w_D)=\left(\frac{B\cdot f}{E},\frac{H\cdot f}{E}\right). \tag{4}$$

Suppose the slope of lines $a'$, $b'$, $c'$ in the image are $k_{-1}$, $k_0$, and $k_1$, respectively, then their general form line equations can be represented as

$$k_iu-w+(w_D-k_iu_D)=0, \tag{5}$$

where $i=-1,0,1$. Comparing Eqs. (3) and (5) associating with Figs. 1(a) and (b), we have

$$k_{-1}\Big/\left(A-\frac{x_c+d_1}{h}C\right)=(-1.0)\Big/\left(G-\frac{x_c+d_1}{h}I\right)$$
$$=(w_D-k_{-1}u_D)\Big/\left[\left(D-\frac{x_c+d_1}{h}F\right)f\right], \tag{6}$$

$$k_0\Big/\left(A-\frac{x_c}{h}C\right)=(-1.0)\Big/\left(G-\frac{x_c}{h}I\right)$$
$$=(w_D-k_0u_D)\Big/\left[\left(D-\frac{x_c}{h}F\right)f\right], \tag{7}$$

$$k_1\Big/\left(A-\frac{x_c-d_2}{h}C\right)=(-1.0)\Big/\left(G-\frac{x_c-d_2}{h}I\right)$$
$$=(w_D-k_1u_D)\Big/\left[\left(D-\frac{x_c-d_2}{h}F\right)f\right]. \tag{8}$$

Let $X_1\triangleq A-\frac{x_c}{h}C$, $X_2\triangleq G-\frac{x_c}{h}I$, $X_3\triangleq\left(D-\frac{x_c}{h}F\right)f$, $X_4\triangleq\frac{C}{h}$, $X_5\triangleq\frac{I}{h}$, $X_6\triangleq\frac{F}{h}f$, substituting them into Eqs. (6), (7) and (8), we can obtain

$$k_{-1}/(X_1-d_1\cdot X_4)=(-1.0)/(X_2-d_1\cdot X_5)$$
$$=(w_D-k_{-1}u_D)/(X_3-d_1\cdot X_6), \tag{9}$$

$$k_0/X_1=(-1.0)/X_2=(w_D-k_0u_D)/X_3, \tag{10}$$

$$k_1/(X_1+d_2\cdot X_4)=(-1.0)/(X_2+d_2\cdot X_5)$$
$$=(w_D-k_1u_D)/(X_3+d_2\cdot X_6). \tag{11}$$

Then, from Eqs. (9), (10), (11), and (4) associating with the definition of the terms of $A$ through $I$ of matrix $M$ in Eq. (1), the expressions can be derived as

$$\frac{X_4}{X_5}\equiv\frac{C}{I}\equiv\tan\psi$$
$$=\frac{k_{-1}(k_1-k_0)(d_1/d_2)+k_1(k_{-1}-k_0)}{(k_0-k_1)(d_1/d_2)+(k_0-k_{-1})}, \tag{12}$$

$$\frac{X_5}{X_6}\equiv\frac{I}{Ff}=$$
$$\frac{(k_0-k_1)(d_1/d_2)+(k_0-k_{-1})}{(k_1-k_0)(k_{-1}u_D-w_D)(d_1/d_2)+(k_{-1}-k_0)(k_1u_D-w_D)}, \tag{13}$$

$$\frac{X_4}{X_6} \equiv \frac{C}{Ff} = \frac{X_5}{X_6} \cdot \frac{X_4}{X_5}, \tag{14}$$

$$\frac{\tan\theta}{\sin\phi} \equiv \frac{BI - CH}{EF}$$

$$\equiv \frac{Bf}{E} \cdot \frac{I}{Ff} - \frac{Hf}{E} \cdot \frac{C}{Ff} = u_D \cdot \frac{X_5}{X_6} - w_D \cdot \frac{X_4}{X_6}. \tag{15}$$

Moreover, as proved in Ref. [5], the vanishing line of the ground plane can be described as

$$u \cdot \sin\psi + w \cdot \cos\psi = -f \cdot \tan\phi. \tag{16}$$

Considering $V_D$ locates on the vanishing line of the ground, then from Eqs. (12) and (16), the vanishing line equation in image plane can be deduced as

$$ku - w + (w_D - ku_D) = 0, \quad k = -X_4/X_5. \tag{17}$$

Let $(u_m, w_m)$ be the image coordinates of the vanishing point of lines with slope $m$ on the ground, we have[5]

$$(u_m, w_m) = \left[\frac{(A + mB)f}{D + mE}, \frac{(G + mH)f}{D + mE}\right]. \tag{18}$$

As shown in Fig. 1(a), its position in the image can be easily obtained by extracting the coordinates of the intersection point $V_0$ between line $d'$ and the vanishing line $\overline{V_D V_0}$ determined by Eq. (17). And from Eqs. (4) and (18), together with the definition of the terms of $A$ through $I$ we have

$$\frac{I}{Ff} \cdot (u_m - u_D) \equiv \frac{I}{Ff} \cdot \left(\frac{A + mB}{D + mE} f - \frac{B}{E} f\right)$$

$$\equiv \cos^2\psi \cdot \frac{\tan\theta}{\sin\phi} \cdot \frac{1}{\sin\theta(\cos\theta - m\sin\theta)}. \tag{19}$$

Then, from Eqs. (12), (13), (15), and (19), together with the known conditions by now we can easily evaluate the value of following expression,

$$X \triangleq \sin\theta(\cos\theta - m\sin\theta)$$

$$= (\tan\theta/\sin\phi) \Big/ \left[(1 + \tan^2\psi) \cdot \frac{I}{Ff} \cdot (u_m - u_D)\right]. \tag{20}$$

Therefore the solution set of Eq. (20) can be derived as

$$\{\theta \,|\theta = k_1\pi + \sin^{-1}[(2X + 1) / \sqrt{1 + m^2}]/2$$

$$-[k_2\pi + \tan^{-1}(1/m)]/2, \quad \text{or}$$

$$\theta = (2k_1 + 1)\pi/2 - \sin^{-1}[(2X + 1)/\sqrt{1 + m^2}]/2$$

$$-[k_2\pi + \tan^{-1}(1/m)]/2,$$

$$k_1, k_2 = \cdots, -1, 0, 1, 2, \cdots, -\pi/2 \leq \theta \leq \pi/2\}. \tag{21}$$

Then from Eq. (15), we have

$$\phi = \sin^{-1}\left[\tan\theta \Big/ \left(u_D \cdot \frac{X_5}{X_6} - w_D \cdot \frac{X_4}{X_6}\right)\right], \tag{22}$$

and from Eqs. (12) and (16) we can obtain

$$\psi = \tan^{-1}(X_4/X_5), \tag{23}$$

$$f = -(w_D \cdot \cos\psi + u_D \cdot \sin\psi)/\tan\phi. \tag{24}$$

So far the calibration of camera focal length and direction parameters are nearly finished, we may have got two or more groups of solutions by different values of $\theta$. By substituting them into Eq. (4), the exact group of the solution can be selected.

Moreover, as shown in Fig. 1, suppose $A_i$ $(i = 1, 2)$ is just the two intersection points of line $d$ with $a$ and $c$ with coordinates $(x_i, y_i, 0)$ on the ground, and $A_i' = (u_i, w_i)$ is the corresponding points in the image, then we have

$$x_2 - x_1 = d_1 + d_2. \tag{25}$$

Substituting Eq. (2) into Eq. (25), we can get

$$h = (d_1 + d_2)/(a - b), \tag{26}$$

where

$$a = (u_1 A + fD + w_1 G)/(u_1 C + fF + w_1 I),$$

$$b = (u_2 A + fD + w_2 G)/(u_2 C + fF + w_2 I).$$

Because position of line $d$ is given beforehand, that means the coordinates of $A_i$ are predetermined, and then the value of $h$ can easily be figured out by equation Eq. (26). So once ground lines $a$, $b$, $c$, and $d$ together with their projection lines $a'$, $b'$, $c'$, and $d'$ in the image plane are determined, value of $h$ computed by Eq. (26) is decided by the calibrated focal length and direction parameters of the camera. Under such conditions, if value of focal length $f$ is supposed to be unchanged, value of $h$ could reflect accuracy of the calibrated directional parameters directly. Therefore we take values of $h$ and $f$ as evaluation parameters to test validity of the calibration method presented in this paper.

Finally, experiments are implemented based on a series of snap shots from real traffic scenes. The authors choose by hand three adjacent lanes with converging point $V_D$ as the set of three parallel lines for calibration, which are labeled with $a'$, $b'$, $c'$ respectively, and the stop line as the line $d'$ with known slope $m = 0$, as shown in Fig. 2. The distance between lines $a$ and $b$ together with that of line $b$ and $c$ is measured beforehand (During the test, we have $d_1 = d_2 = 3.25$ m).

The calibration results show that the calibration parameters have close relationship with the accuracy of the four lines choice, but robust results could be achieved with a calibration error of about 5% in average by carefully selected lines. The robust average values of the calibrated focal length and height of camera lens center during the test are listed in Table 1, where the column "offset" specifies the percentage difference of the computed parameter to the real value.


Fig. 2. A snapshot of traffic scenes and the selected calibration target.

**Table 1. Experimental Result of Camera Focal Length and Lens Center Height**

| Parameter | Computed Value | Real Value | Offset (%) |
|---|---|---|---|
| Focal Length (pixel) | 665.43 | 700.00 | 4.94 |
| Lens Center Height (m) | 4.87 | 5.10 | 4.51 |

Considering camera parameters is calibrated by a series of analytical equations, whose deduction is correct, so the method itself is accurate and its precision is only decided by accuracy of the calibration target selection. It can be concluded that most of calibration error during the experiments comes from the manual means of lines selection. Therefore, the obtained calibration error above could not completely show actual potential of the proposed method, but in some sense it can prove its validity. To promote accuracy of the approach for further improvements, the nearer future work is to develop robust four lines selection method from traffic images with optimized direction extraction of the calibration lines and accurate position estimate of the converging vanishing point among the three parallel lines. Then various works of detailed video traffic analysis can be performed as further steps based on camera parameters gained by the proposed method.

This work was supported by the auspice of National Key Project for Basic Research on Urban Traffic Monitoring and Management System, PRA SI01-01, G1998030408. Z. Chen's e-amil address is chenzhaoxue@sjtu.edu.cn.

## References

1. Z. X. Chen and P. F. Shi, Chin. Opt. Lett. **1,** 585 (2003).
2. N. H. C. Yung, G. K. H. Pang, and G. S. K. Fung, *Proc. 7th World Congress on Intelligence Transportation Systems* 3024 (2000).
3. R. Y. Tsai, IEEE J. Robotics and Automation **RA-3,** 323 (1987).
4. E. K. Bas and J. D. Crisman, in *Proceedings of IEEE Conference on Intelligent Transportation Systems* 362 (1997).
5. L. L. Wang and W. H. Tsai, IEEE Trans. Pattern Analysis and Machine Intelligence **13,** 370 (1991).